E. FEDOROV

rong anomalies of the atmospheric
turbations in the conductivity of the
d mechanisms: Galvanic and heated,
lvanic mechanism is responsible for
on. The Joule heating causes an rise
ads to magnification of the electron
conductivity reduction. The estima-
ible in comparison with the second

here could give reasonable explana-
lies observed before strong earth-
ced conductivity can be responsible
o mode into another normal modes
mode but with shifted phase)[11],

press his thanks to Prof. O. Molchanov
his helpful comments on this paper.

-188, 1976.
85.
GA General Assembly, Wellington, New

sikalni vlastnosti hornin a jejich vyuzit v

urn. of Atmospheric Electricity, **16**, 259–

tmosphere, Edward Arnold, 1975.

here, Springer-Verlag, New-York, 1978.
. S. Yampolsky, *Pub. Inst. Geophys. Pol.*

awai, *J. Phys. Earth*, **44**, 413–418, 1996
mena Related to Earthquake Prediction,
, Tokyo, 391–407, 1994.

Atmospheric and Ionospheric Electromagnetic Phenomena Associated with Earthquakes,
Ed. M. Hayakawa, pp. 597–617.

Statistical Study of Ionospheric Plasma Response to Seismic Activity: Search for Reliable Result from Satellite Observations

V. V. AFONIN[1,2], O. A. MOLCHANOV[2], T. KODAMA[2], M. HAYAKAWA[3], and O. A. AKENTIEVA[1]

[1]*Institute of Space Research RAS, Moscow, Russia*
[2]*EORC/NASDA, Tokyo, Japan*
[3]*The University of Electro-Communications, Chofu, Tokyo, Japan*

Abstract. Using a rather large data base of plasma density recording on board a Russian satellite Intercosmos 24 (more than 7000 hours over the world), we discovered a reliable correlation between the global distribution of seismic activity and ion density variations. The best parameters to find a significant correlation between the two, are normalized standard deviation (NSD) and relative normalized standard deviation (RNSD). Maximal values of ion density NSD correlated with seismic activity are 10–15%. Clear correlation is found only for day time conditions (10–16 LT) and altitude range above the main ionospheric maximum (heights 500–700 km). This correlation disappears during night time conditions and during magnetic storms. Preliminary analysis of similar data collected on the Cosmos-900 satellite, shows the same type of correlation.

1. Introduction

There have been published many papers on seismogenic effects observed on board satellites, including the recording of electromagnetic wave emissions, energetic particle fluxes, ion/electron density, magnetic field variations, ion composition and so on (see e.g. a comprehensive monograph compiled by Hayakawa and Fujinawa, 1994 and some recent reviews by Molchanov, 1993 and Hayakawa, 1996). Especially intriguing are the reports on precursory signatures in such registrations, implying a possibility of earthquake prediction. However, till now there is no proof of reliability of these results, and furthermore the mechanisms of seismicity-ionosphere coupling are poorly understood. We know that there are a lot of natural perturbations in ionospheric plasma, connected with magnetic storms, particle precipitation from radiation belts etc., which could be misinterpreted as seismogenic events. Consequently there are a lot of doubts on the existence of effective seismic influence on the ionospheric plasma. This problem could be formulated in a more definite and almost practical manner: is it possible to prove that plasma/wave measurements on board low-orbital satel-

lites can be considered as a reliable indicator of seismic activity on the ground? It is the main target of our research, and our initial results are reported here.

2. Main Strategy of Research and Description of Data

The basic idea of all the previous researches is to analyze the data around the time of any rather big earthquake and above its epicenter in order to demonstrate these data are different from those obtained in other places and times. It is so-called case study. Sometimes we are so lucky to find this signature but it is very difficult to prove that we have a seismogenic effect, but not coincidental plasma burst phenomenon. Because we need to have data set either continuous in space at a fixed time or otherwise continuous in time at a fixed place to use the conventional statistic methods. Of course, we could use the data from geostationary satellites for investigation of the second possibility, but such data seem to be contaminated by very strong magnetospheric variations usually present in auroral regions. So, if we use the data from low-orbital satellites, we have an intrinsic incompatibility of our data with statistical requirements for a case study. It means we need to seek some other approaches.

The main idea of our strategy is to use an inhomogeneity of seismic activity distribution over the Earth. The situation is depicted in Fig. 1. It is well known that seismic activity in any rather long period of time is concentrated along the so-called plate boundaries. So, if seismic activity influences the ionosphere indeed, we should find the statistically valuable and similar space inhomogeneity in our data after their averaging over the time. Of course, it is desirable to have rather large data base and to analyze the parameter whose divergence in space is not fast in comparison with the characteristic time of usual earthquake sequences. As we discussed in our related research (Molchanov *et al.*, 1997), the duration of earthquake sequence or earthquake pattern is from a few days to a few weeks in a region about 100 km. The only plasma parameter which is conserved in this space scale for a long time is the density of cold plasma, whose estimated velocity of magnetic drift is about 0.01–0.1 m/s at the altitude ~1000 km and life time in magnetic tube with cross-section about 100 km is 10–100 days. Therefore we selected the data of ion density and temperature obtained on Russian satellites Intercosmos-24 (Aktivny) during its operation from October 1989 to December 1992, and Cosmos-900. The characteristics of these satellites are presented in Table 1, the description of measured parameters is given in Table 2, and the device itself is shown in Fig. 2. We have analyzed only the data received in memory regimes ZAP-3 and ZAP-4, because the time and space resolution in the slow mode ZAP-4 (2.5 sec and 18 km correspondingly) is enough for our requirements. The examples of data are demonstrated in Figs. 3–5. Upper line in Fig. 3 is the ion density in linear scale on the right in units of 10^3 cm^{-3} and lower line is the plasma temperature (left scale in K degrees). The data (29.12.1989) and universal time (from 15.20.40 UT to 16.18.23 UT) are shown above the picture.

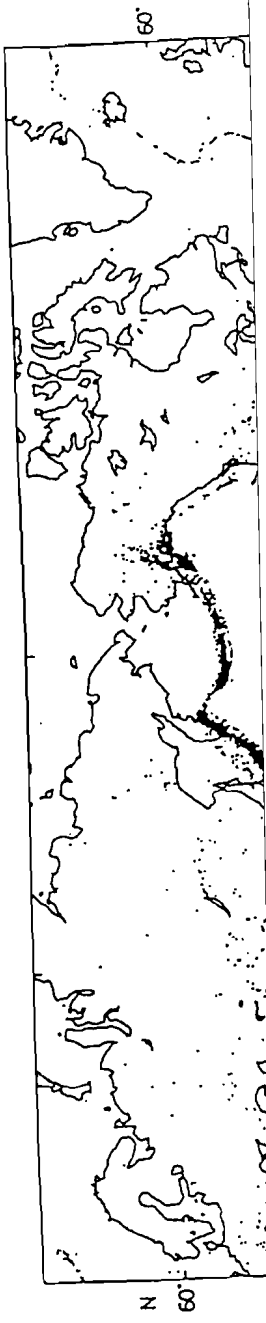

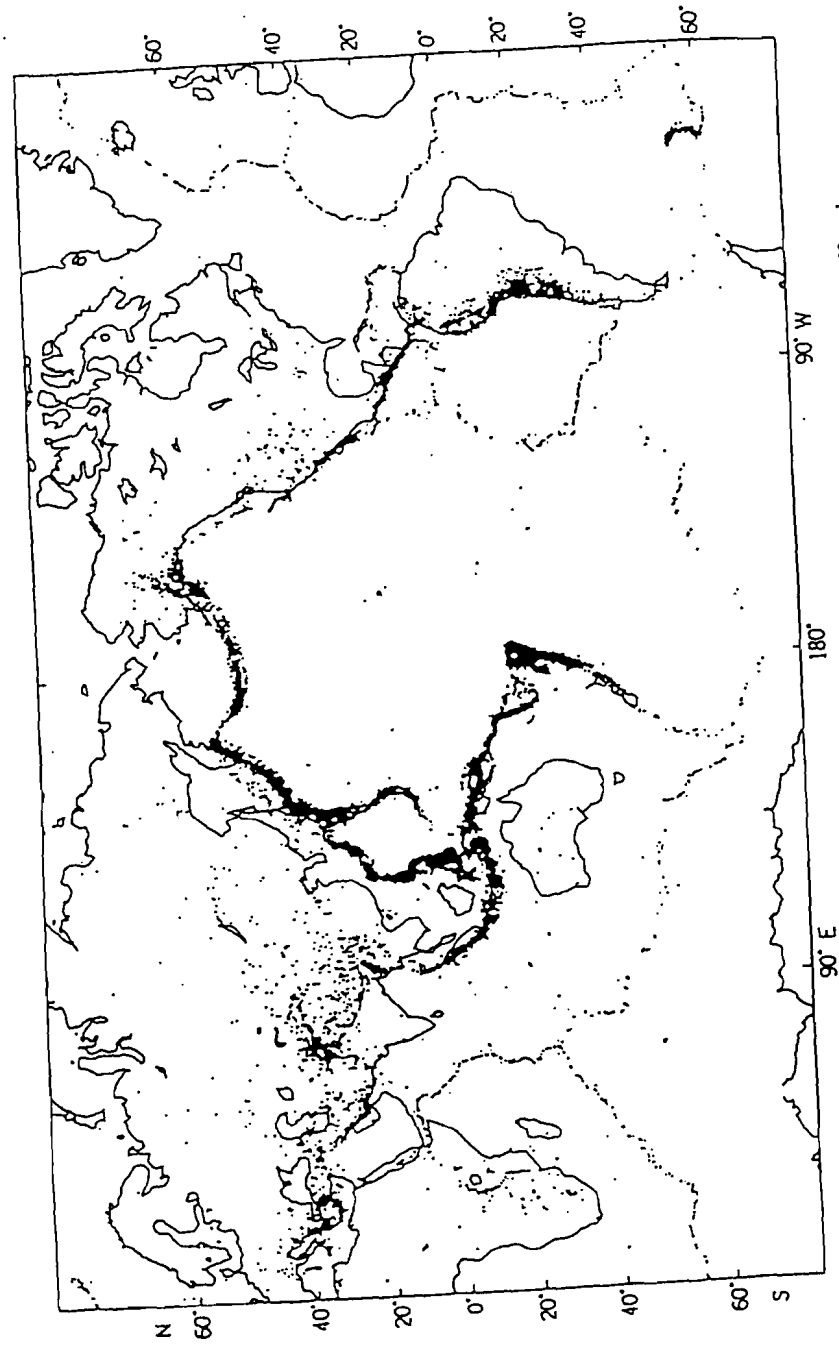

Fig. 1. Worldwide distribution of earthquakes of M 4.5 and larger that occurred between 1963 and 1977 (according to the U.S. National Oceanic and Atmospheric Administration (NOAA) (1983)).

l.

of seismic activity on the ground? nitial results are reported here.

of Data

es is to analyze the data around the epicenter in order to demonstrate n other places and times. It is so- to find this signature but it is very ffect, but not coincidental plasma ata set either continuous in space ime at a fixed place to use the ould use the data from geostation- ssibility, but such data seem to be ariations usually present in auroral al satellites, we have an intrinsic irements for a case study. It means

inhomogeneity of seismic activity icted in Fig. 1. It is well known that ime is concentrated along the so- influences the ionosphere indeed, milar space inhomogeneity in our urse, it is desirable to have rather ose divergence in space is not fast sual earthquake sequences. As we ov *et al.*, 1997), the duration of from a few days to a few weeks in ameter which is conserved in this plasma, whose estimated velocity altitude ~1000 km and life time in km is 10–100 days. Therefore we ure obtained on Russian satellites n from October 1989 to December f these satellites are presented in eters is given in Table 2, and the nalyzed only the data received in the time and space resolution in the rrespondingly) is enough for our nstrated in Figs. 3–5. Upper line in right in units of 10^3 cm^{-3} and lower legrees). The data (29.12.1989) and 3 UT) are shown above the picture.

Below the main orbital information is given: number of cadre (measurement point), altitude (in km), invariant (geomagnetic) latitude (Φ), magnetic local time (MLT), geographic latitude (φ), geographic longitude (λ), magnetic L-parameter and some solar parameters. It is evident that large fluctuations in density and temperature appear only at the high-latitude part of the orbit, φ, $\Phi > 50°$ in this case. The same behavior is observed in another example depicted in Fig. 4. We can also note that the near-apogee data ($H \sim 1500$–2000 km) are usually much more variable in comparison with the data near the perigee ($H \sim 500$–800 km) even if both are at the low-latitude regions. The results of continuous 18.5 hour measurements are shown in Fig. 5 (about 10 full orbits). It is obvious that unlike high-latitude and high-altitude parts of the orbits the data are rather similar and regular to be used for our statistical studies.

Table 1. Main characteristics of the satellites.

Satellite	INTERCOSMOS-24 (ACTIVNYI)	Cosmos-900
Orbit type	Elliptical polar	Circular polar
Apogee	2497 km	523 km
Perigee	511 km	508 km
Inclination	82.6°	82°
Orbit period	124 min	94 min
Date of launch	September 28, 1989	April 30, 1977
Active life time	≈ 3 years	≈ 2.5 years
Number of data available (in orbit)	≈ 3500	≈ 1800

Onboard memory mode and max length of record	Sampling time of 1 TM channel	Worst resolution for N_i measurements		
		in time	in space	in latitude
ZAP-1 (5 min)	0.01 s			
ZAP-2 (30 min)	0.08 s			
ZAP-3 (120 min)	0.32 s			
ZAP-4 (19 hours)	5.12 s	2.5/1.0 * sec	18/7.5 * km	0.2/0.07 * deg

Table 2. Ionospheric Plasma Spectrometer.

(IPHP)

Objective: Complex measurements of major parameters of ionospheric aimed at:

- regular monitoring of ionosphere behavior
- complex study of different physical phenomena in ionosphere

IPHP consist of

1. Retarding Potential Analyzer - RPA-X - ram direction
2. Retarding Potential Analyzer - RPA-Z - zenith direction
3. Electron Temperature Sensor - TE-X - ram direction
4. Electron Temperature Sensor - TE-Y - East-West direction
5. Electron Temperature Sensor - TE-Z - zenith direction
6. Drift Meter - DM - ram direction

Measured parameters:

Ion density	- Ni	- $10^1 \ldots 5*10^6$ cm^{-3}
Ion temperature	-Ti	- 300...15,000 K
Major ion masses	- Mi	- 1,4,16 a.m.u.
Electron temperature	- Tex	- 700...80,000 K
Te anisotropy	- Tey, Tez	- 700...80,000 K
Ion drift velocity	- Vdx, Vdy	- 0.1...12 km/s

Vertical ion flux (E ≤ 50 eV) - ≥ $1.5 \cdot 10^6$ cm^{-2}sec^{-1}... $1.5 \cdot 10^{10}$ cm^{-2}sec^{-1}

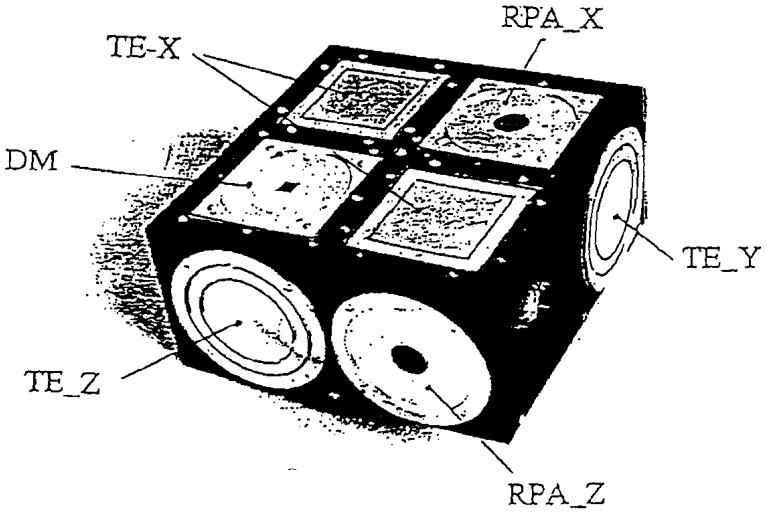

Fig. 2. Scheme of device IPHP, which was installed on the satellites.

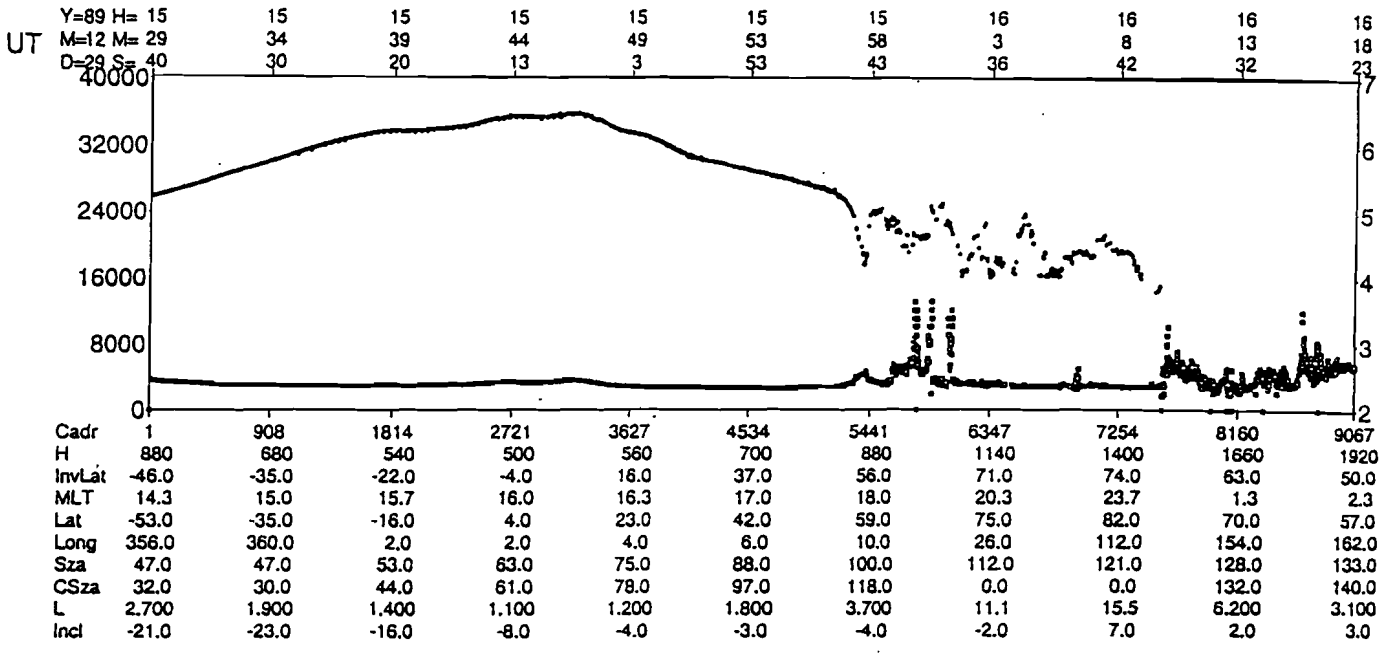

Fig. 3. Example of IPHP data,obtained on satellite Intercosmos-24 on 29 Dec. 1989. Time (UT) is shown above. Upper line in the picture is the value of ion density, whose scale is shown on the right ($\times 10^3$ cm^{-3}). Lower line is the electron temperature, whose scale is shown on the left (in K degree). Below the orbital parameters are given (see text). There is the memory regime ZAP-3 (sampling rate 0.32 s, Table 1).

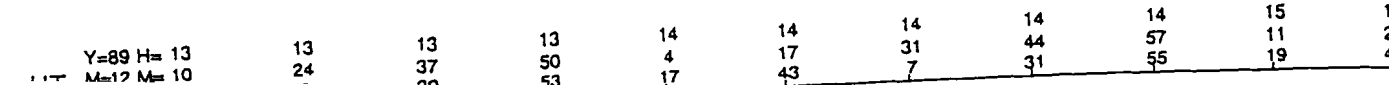

Lat	-53.0	-35.0	-16.0	4.0	23.0	42.0	59.0	75.0	82.0	2.3
Long	356.0	360.0	2.0	2.0	4.0	6.0	10.0	26.0	112.0	57.0
Sza	47.0	47.0	53.0	63.0	75.0	88.0	100.0	112.0	121.0	70.0
CSza	32.0	30.0	44.0	61.0	78.0	97.0	118.0	0.0	0.0	154.0
L	2.700	1.900	1.400	1.100	1.200	1.800	3.700	11.1	15.5	128.0
Incl	-21.0	-23.0	-16.0	-8.0	-4.0	-3.0	-4.0	-2.0	7.0	132.0
										6.200
										2.0

Fig. 3. Example of IPHP data,obtained on satellite Intercosmos-24 on 29 Dec. 1989. Time (UT) is shown above. Upper line in the picture is the value of ion density, whose scale is shown on the right ($\times 10^3$ cm^{-3}). Lower line is the electron temperature, whose scale is shown on the left (in K degree). Below the orbital parameters are given (see text). There is the memory regime ZAP-3 (sampling rate 0.32 s, Table 1).

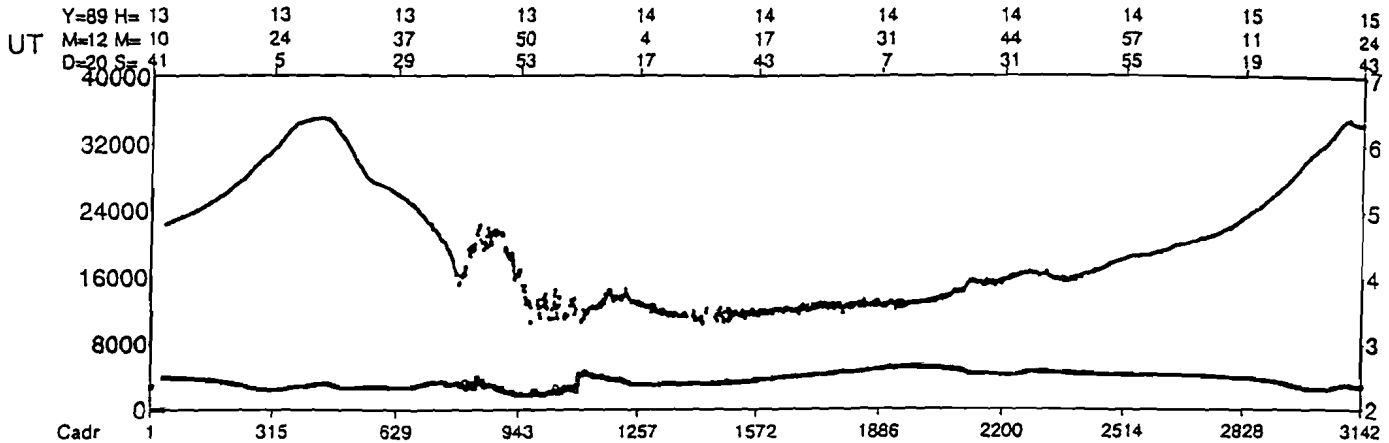

Cadr	1	315	629	943	1257	1572	1886	2200	2514	2828	3142
H	1240	620	560	1100	1800	2340	2500	2280	1700	960	520
InvLat	-58.0	-15.0	40.0	75.0	43.0	9.0	-23.0	-53.0	-67.0	-42.0	3.0
MLT	15.0	17.0	18.0	23.3	4.0	5.0	5.7	6.7	12.0	16.0	17.3
Lat	-56.0	-8.0	45.0	81.0	43.0	7.0	-26.0	-58.0	-81.0	-41.0	10.0
Long	44.0	50.0	56.0	170.0	214.0	218.0	218.0	224.0	336.0	18.0	22.0
Sza	55.0	71.0	100.0	122.0	123.0	109.0	91.0	73.0	58.0	58.0	80.0
CSza	37.0	69.0	107.0	0.0	142.0	118.0	79.0	57.0	0.0	42.0	81.0
L	4.700	1.200	1.800	17.6	2.400	1.400	1.600	3.700	8.400	2.400	1.100
Incl	-42.0	-7.0	4.0	19.0	16.0	11.0	15.0	35.0	-10.0	-25.0	-2.0

Fig. 4. Another example of Intercosmos-24 data on 20 Dec. 1989 (ZAP-4 regime). See the explanation in Fig. 3.

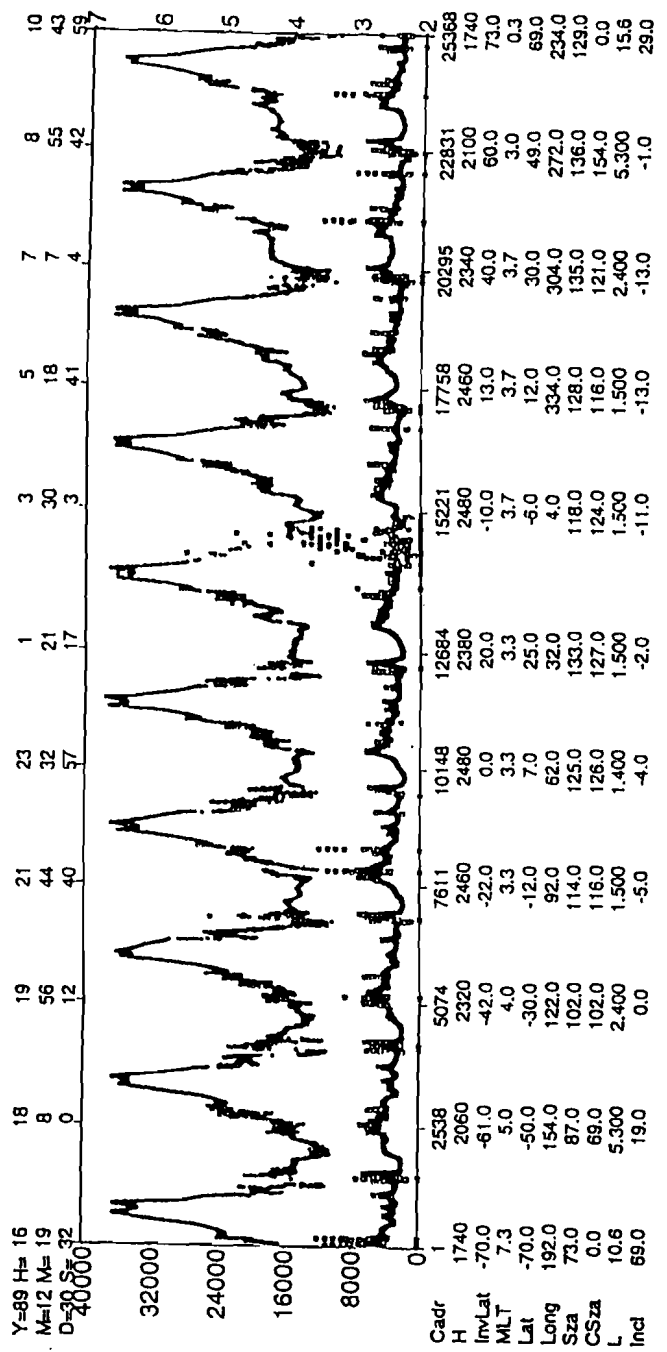

Fig. 5. Another example of Intercosmos-24 data on 30 Dec. 1989 (ZAP-4 regime). See explanation in Fig. 3.

3. Main Results of

We selected th

1. Geograph

45 divisions.

2. Geograph

3. Local tim

LT; day 10–16 LT

4. Altitude

= 20 divisions.

5. Index of

activity $3 \le K_p \le 5$

Thus, we organize

"cells". The whol

orbits. It means th

which seems as su

Of course, we cou

the seasonal subdi

to the failure of s

In each elem

a. Average

b. Standar

c. Normal

d. Relativ

RNSD

where <NSD> is

K_p parameters an

cal perturbations

chosen: 2-D map

will be shown a

(A) Map presen

First of all

correlation with

of averaged val

in a range of H

the operation

shows a place w

is rather simila

features of wel

resemblance w

of RNSD para

7. The similar

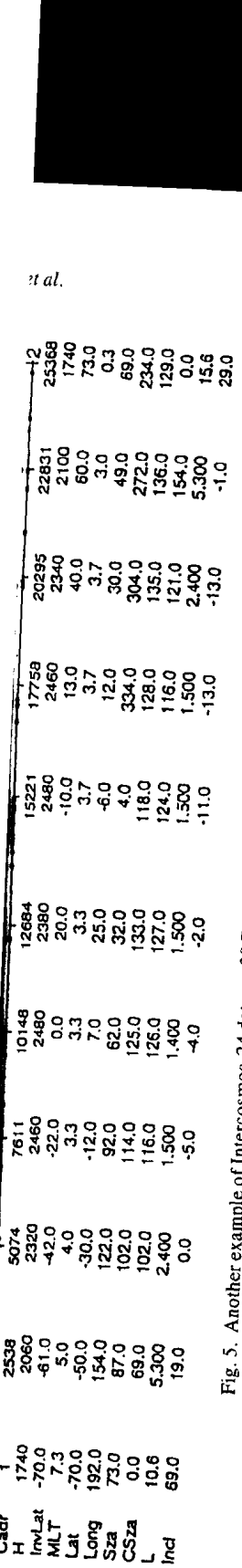

Fig. 5. Another example of Intercosmos-24 data on 30 Dec. 1989 (ZAP-4 regime). See explanation in Fig. 3.

3. Main Results of Statistical Study

We selected the following basic parameters of our recording:

1. Geographic latitude φ; choose the division $\Delta\varphi = 4^\circ$, and resulting $N_\varphi =$ 45 divisions.
2. Geographic longitude λ; $\Delta\lambda = 5^\circ$, $N\lambda = 72$.
3. Local time LT; chosen at 4 grades: night, 22–04 LT; morning, 04–10 LT; day 10–16 LT; evening, 16–22 LT, resulting in $N(\mathrm{LT}) = 4$.
4. Altitude H, $\Delta H = 100$ km, in a range 500 km–2500 km, resulting in $N(H)$ = 20 divisions.
5. Index of magnetic activity K_p; 3 grades: quiet activity $K_p < 3$, medium activity $3 \le K_p \le 5$, strong activity, $K_p > 5$, resulting in $N(K_p) = 3$.

Thus, we organized $N = N_\varphi \cdot N_\lambda \cdot N(H) \cdot N(\mathrm{LT}) \cdot N(K_p) = 7.776 \cdot 10^5$ elementary "cells". The whole volume of our data base is about 10^7points or about 3500 orbits. It means that in each elementary cell we found about $N_c = 10$–30 points, which seems as sufficient for reasonable averaging in the selected configuration. Of course, we could perform a more detailed division, for example, introducing the seasonal subdivisions or taking some atmospheric parameters but it could lead to the failure of statistics.

In each elementary cell we calculated the following values:

a. Average value $n = \sum n_i / N_c$.
b. Standard deviation value: $\mathrm{SD} = (\sum (n_i - n)^2 / N_c)^{1/2}$.
c. Normalized standard deviation value: $\mathrm{NSD} = \mathrm{SD}/n$.
d. Relative standard deviation value:
$\mathrm{RNSD} = \mathrm{NSD}/\langle \mathrm{NSD} \rangle$,

where <NSD> is the averaging over a "map" or all the cells with equal LT, H and K_p parameters and with some limitation of latitude in order to exclude geophysical perturbations at high latitudes. Two types of presentation of the results were chosen: 2-D map presentation and longitudinal dependence. Now some pictures will be shown and discussed.

(A) Map presentation

First of all we found that only RNSD could be helpful for estimating a correlation with seismic activity. As an example, Fig. 6 illustrates the distribution of averaged values n above $n_i = 0.93\, n_{i\,\max}$ ($n_{i\,\max}$ is maximal value over the map) in a range of $H = 500$–600 km during day. Distribution of seismic activity during the operation of Intercosmos-24 satellite is presented by circles. Each circle shows a place where a rather large earthquake ($M > 5$) occurred. This distribution is rather similar to that shown in Fig. 1. Indeed, density distribution has all the features of well-known equatorial anomaly of ionospheric plasma and has no any resemblance with the distribution of earthquakes. But now let us see a distribution of RNSD parameter in the same situation, $H = 500$–600 km, LT = 10–16 in Fig. 7. The similarity is much more pronounced. Of course, it is one of the best

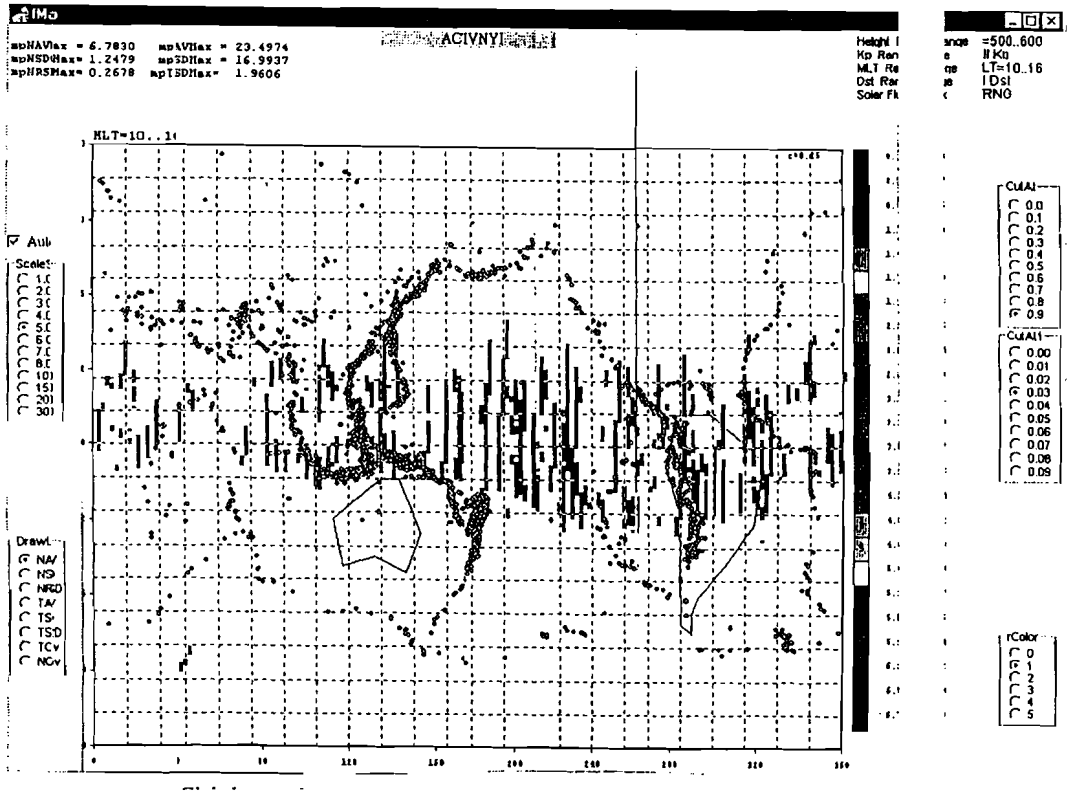

Fig. 6. Global map of ion density distribution (Only $N_i > 093N_i$ max). Satellite Intercosmos-24 (Aktivny).

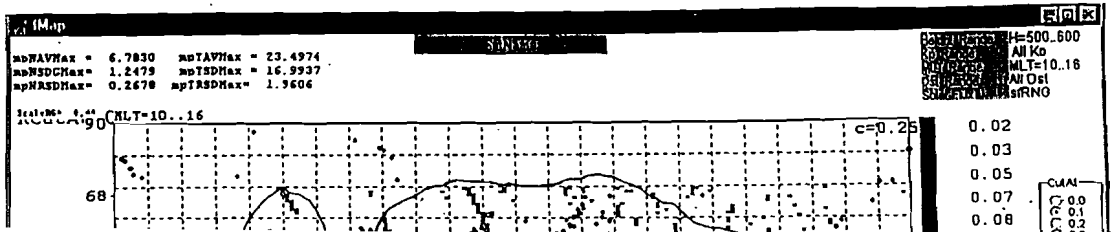

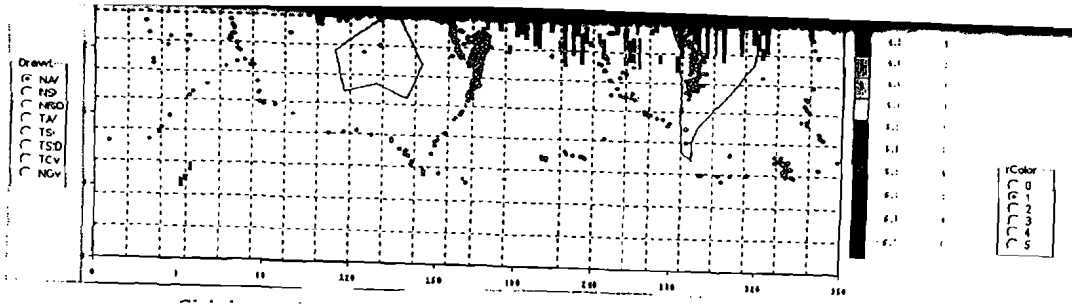

Fig. 6. Global map of ion density distribution (Only $N_i > 093N_i$ max). Satellite Intercosmos-24 (Aktivny).

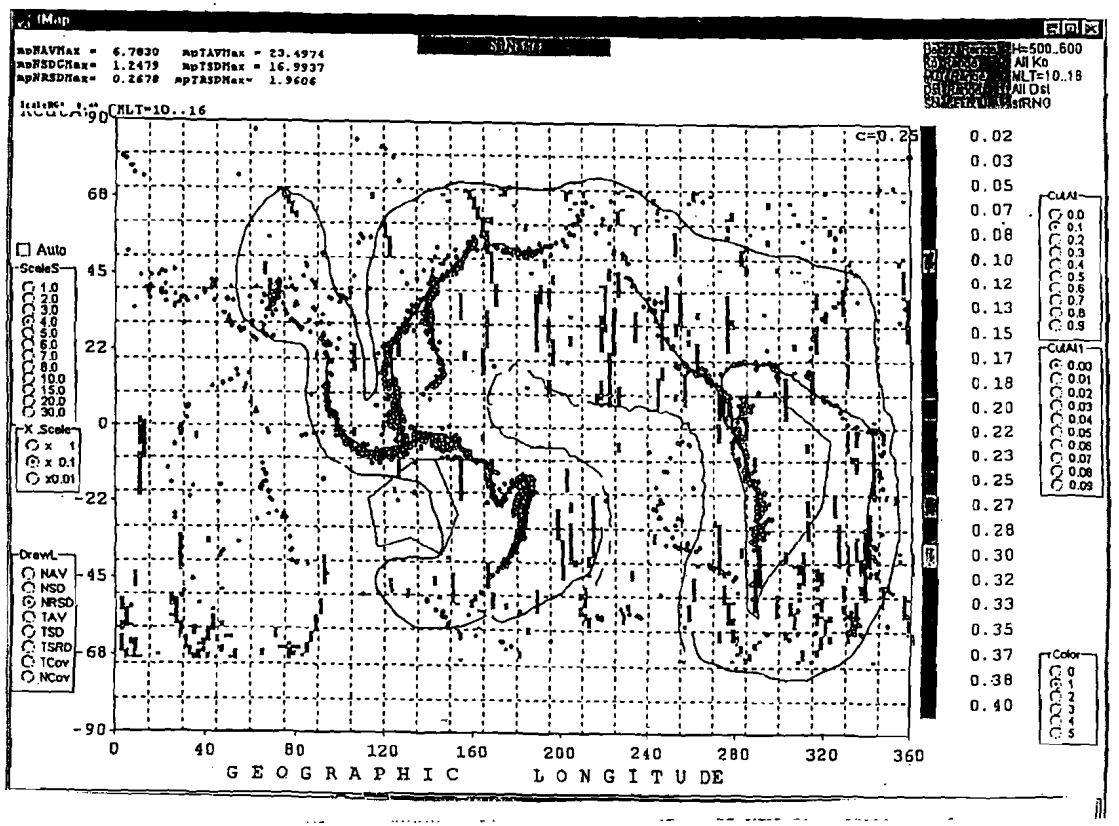

Fig. 7. Global distribution of earthquakes during the operation time of Intercosmos-24 (1989–1990 years) and distribution of RNSD of ion density above 2σ level.

examples. We analyzed all the possible maps and only in a few of them we could find out this type of similarity on the following conditions:

a. Altitude H is near the perigee, $500 < H < 800$ km.

b. Geographic latitude φ or geomagnetic latitude Φ is limited, $|\varphi|, |\Phi| < 50^\circ$.

c. Only day time period, LT = 10–16 LT.

d. Only geomagnetically quiet periods, $K_p < 3$.

Even after such a selection the correlation envisage from the maps was not so convincing. Furthermore, it was difficult to estimate quantitatively this correlation.

(B) Longitudinal dependence presentation

So, we finally analyzed only the longitudinal dependence of both RNSD and seismic activity. Such a plot is shown in Fig. 8. The top panel is the number of large earthquakes during all the period of our observation, averaged over latitude. The bottom panel is the map presentation already discussed. In the center of Fig. 8 the RNSD also averaged over latitude is demonstrated by a solid line and longitudinal dependence of earthquake occurrence is repeated by a thin line. In correspondence with the known criteria we can believe that if RNSD >2 then the probability of random fluctuation is low (it is famous 2σ statistical criteria in our case). In the plot which is demonstrated in Fig. 8, we cannot find out any significant correlation, because all the values of RNSD < 2. We can explain this negative result with too big margin of altitudes, $H = 500$–1000 km, selected here. Positive result for an altitude range $H = 600$–700 km is found in Fig. 9. It is evident that exceeding the 2σ level happened just in a region above the enhanced seismic activity area, and furthermore, a clear peak to peak correlation can be noted. This good correlation is not altered even if we consider only earthquakes with $M > 5.3$ (Fig. 10). With this criterion the number of earthquakes is decreased by about 3 times, but their correlation with density variations is the same. Then we have tried to understand whether seismo-ionospheric coupling is controlled geographically or geomagnetically. At first we have tried to compare our results both in the geographic and geomagnetic coordinates. However, we have found that the results are similar for a narrow altitude range, but for enlargement of altitude range, when geomagnetic coordinates would be more perspective, we have "smoothing" of the effect. It was already shown in Fig. 8, which was plotted just in geomagnetic coordinates. So, we have chosen another way. Longitudinal dependence of seismic occurrence and RNSD is shown in Fig. 11 only for northern hemisphere. Increase of density variations at the longitudes 0–10° and at the range $\lambda \sim 310$–320° is possibly related with magnetic anomalies in Africa and Brazil, but increase of RNSD in the center of plot ($\lambda \sim 110$–150°) is no doubt related with seismic activity. Unlike it the density variations in the southern hemisphere do not correlate with seismic activity in the same hemisphere (Fig. 12), but they are rather well correlated with seismic activity in the opposite,

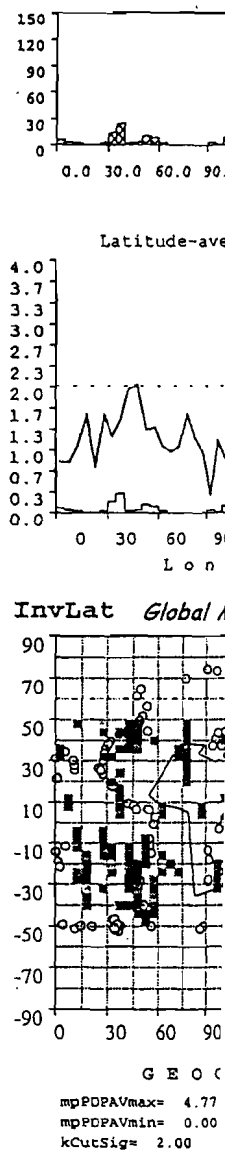

Fig. 8. Longitudinal dep
and longitudinal vari
(solid line in a cente

s and only in a few of them we could
wing conditions:
$0 < H < 800$ km.
netic latitude Φ is limited, $|\varphi|$, $|\Phi| <$
6 LT.
ds, $K_p < 3$.
envisage from the maps was not so
estimate quantitatively this correla-

dinal dependence of both RNSD and
g. 8. The top panel is the number of
observation, averaged over latitude.
ready discussed. In the center of Fig.
s demonstrated by a solid line and
urrence is repeated by a thin line. In
can believe that if RNSD >2 then the
is famous 2σ statistical criteria in our
in Fig. 8, we cannot find out any
es of RNSD < 2. We can explain this
des, $H = 500$–1000 km, selected here.
700 km is found in Fig. 9. It is evident
a region above the enhanced seismic
o peak correlation can be noted. This
nsider only earthquakes with $M > 5.3$
earthquakes is decreased by about 3
ations is the same. Then we have tried
coupling is controlled geographically
to compare our results both in the
However, we have found that the
nge, but for enlargement of altitude
uld be more perspective, we have
own in Fig. 8, which was plotted just
chosen another way. Longitudinal
NSD is shown in Fig. 11 only for
ariations at the longitudes 0–10° and
d with magnetic anomalies in Africa
ter of plot ($\lambda \sim 110$–150°) is no doubt
e density variations in the southern
ctivity in the same hemisphere (Fig.
ith seismic activity in the opposite,

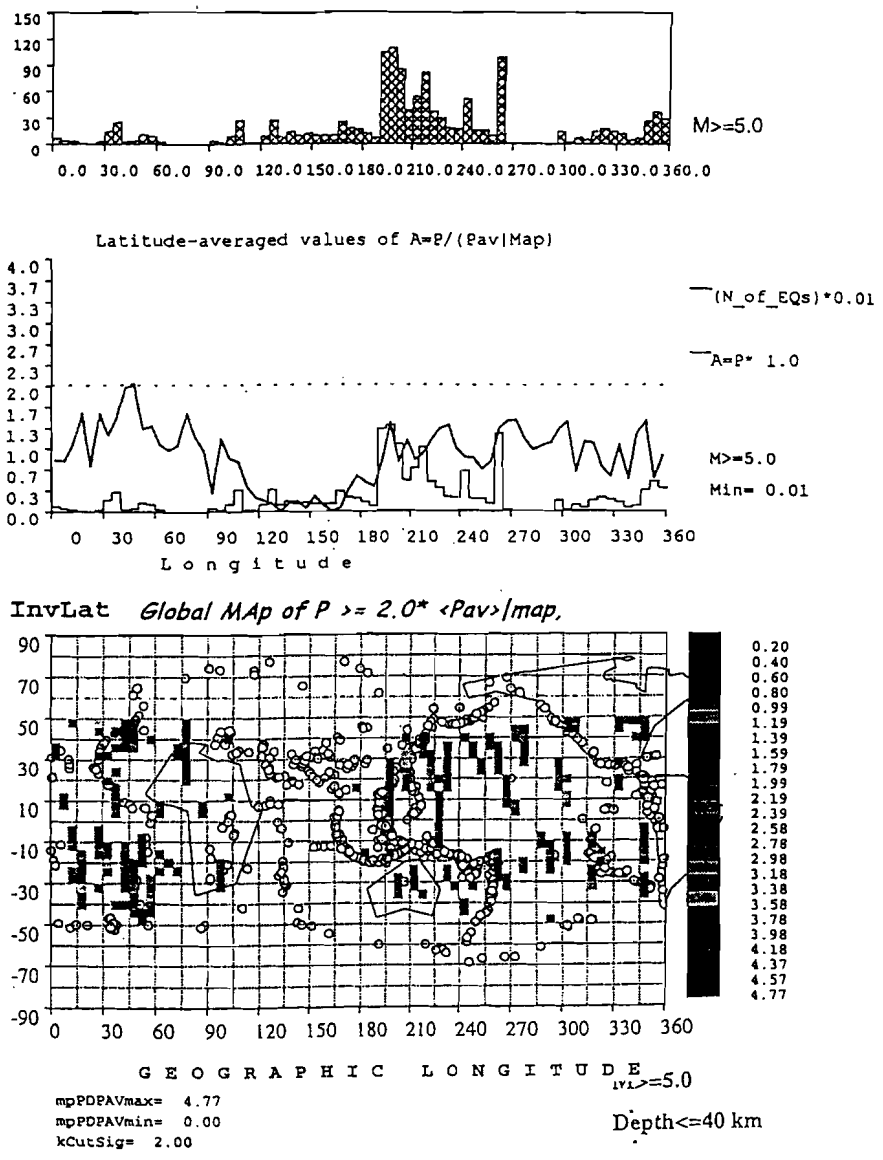

Fig. 8. Longitudinal dependence of earthquake occurrence rate ($M > 5$, 1989–1990 years) (above), and longitudinal variation of RNSD of density, $H = 500$–1000 km, $K_p < 3$, LT = 10–16, $|\Phi| < 50^\circ$ (solid line in a center). Map of earthquakes and RNSD >2 for the same conditions (below).

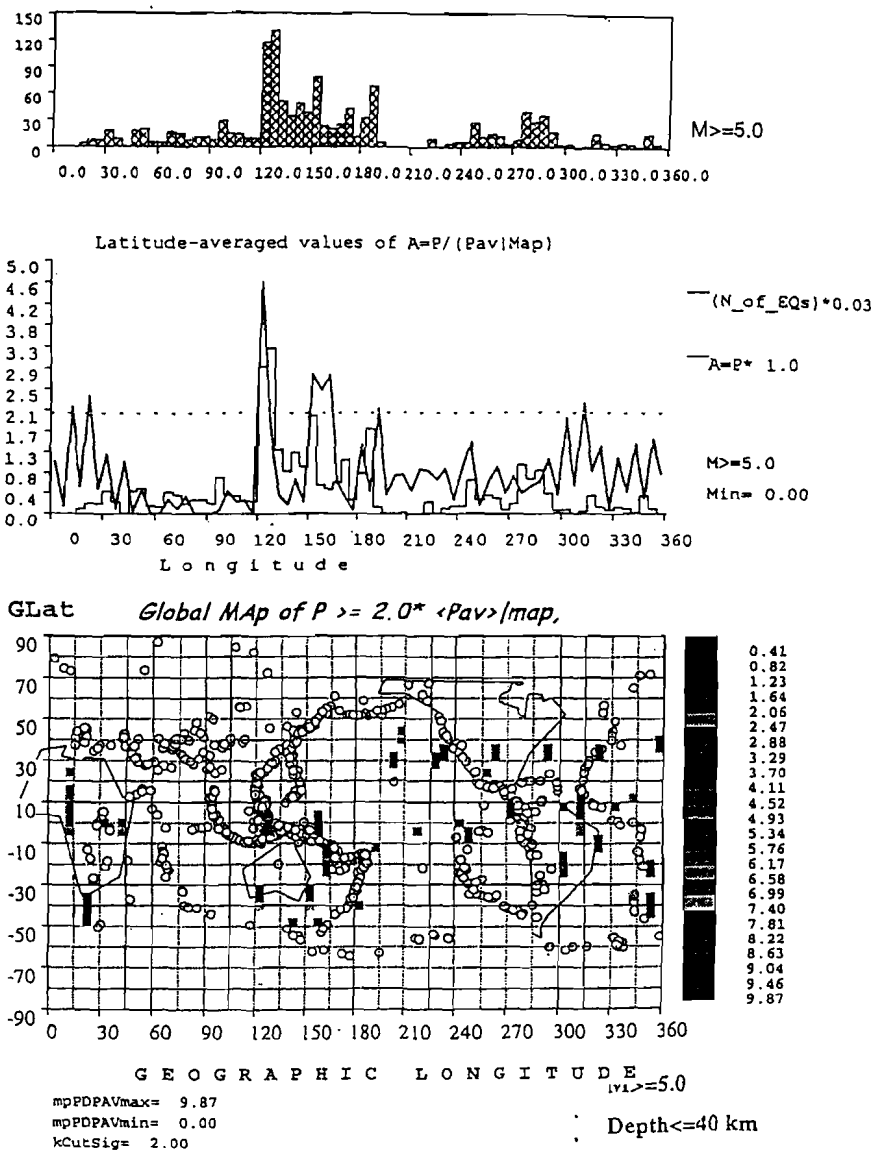

Fig. 9. The same as Fig. 8, but for H = 600–700 km and for the geographic coordinates.

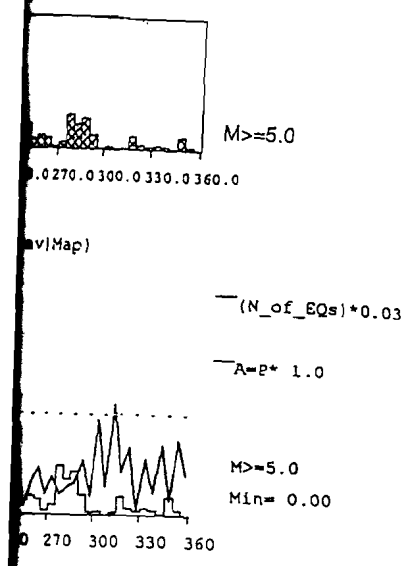

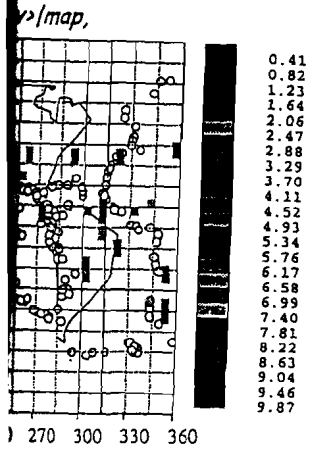

0 km and for the geographic coordinates.

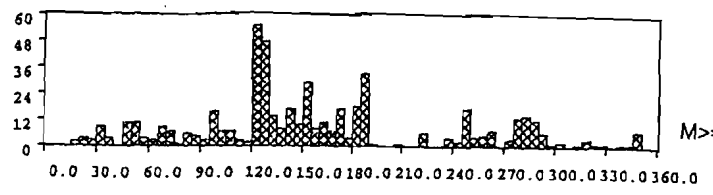

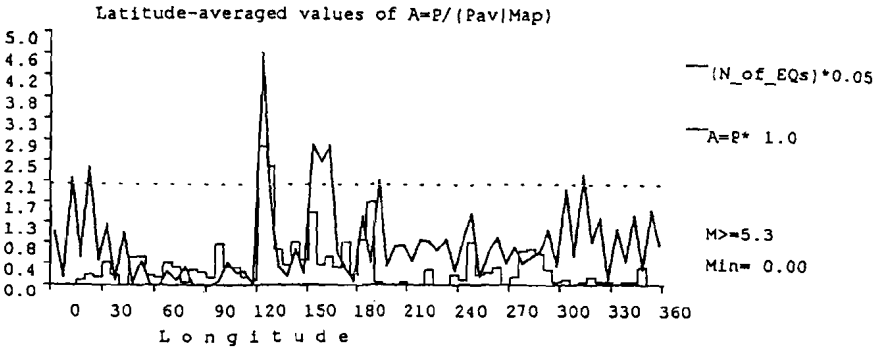

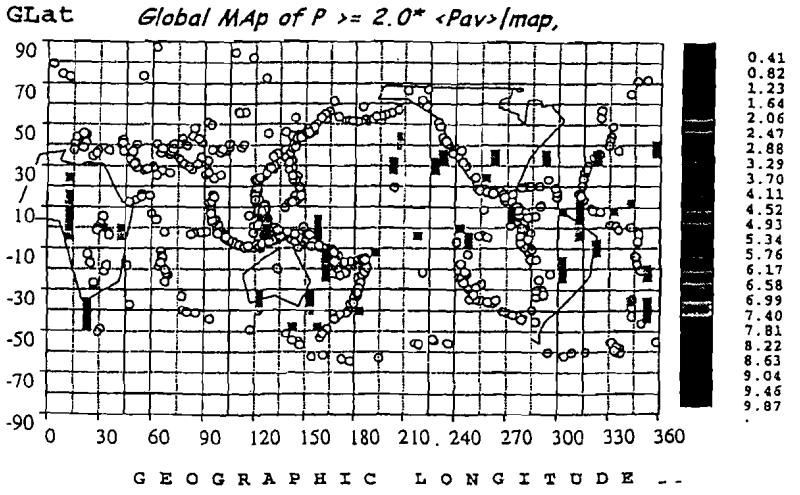

Fig. 10. The same as in Fig. 9, but for larger earthquakes (M > 5.3).

northern hemisphere (Fig. 13). The simplest explanation of the facts presented in Figs. 11–13 is that variations in the southern hemisphere are mainly controlled by northern seismic activity, and thus, we need to assume an essential coupling along the magnetic field line or geomagnetic control.

To check the results obtained on board the Intercosmos-24 satellite we have performed the similar analyses of data from Cosmos-900 satellite. Though we are

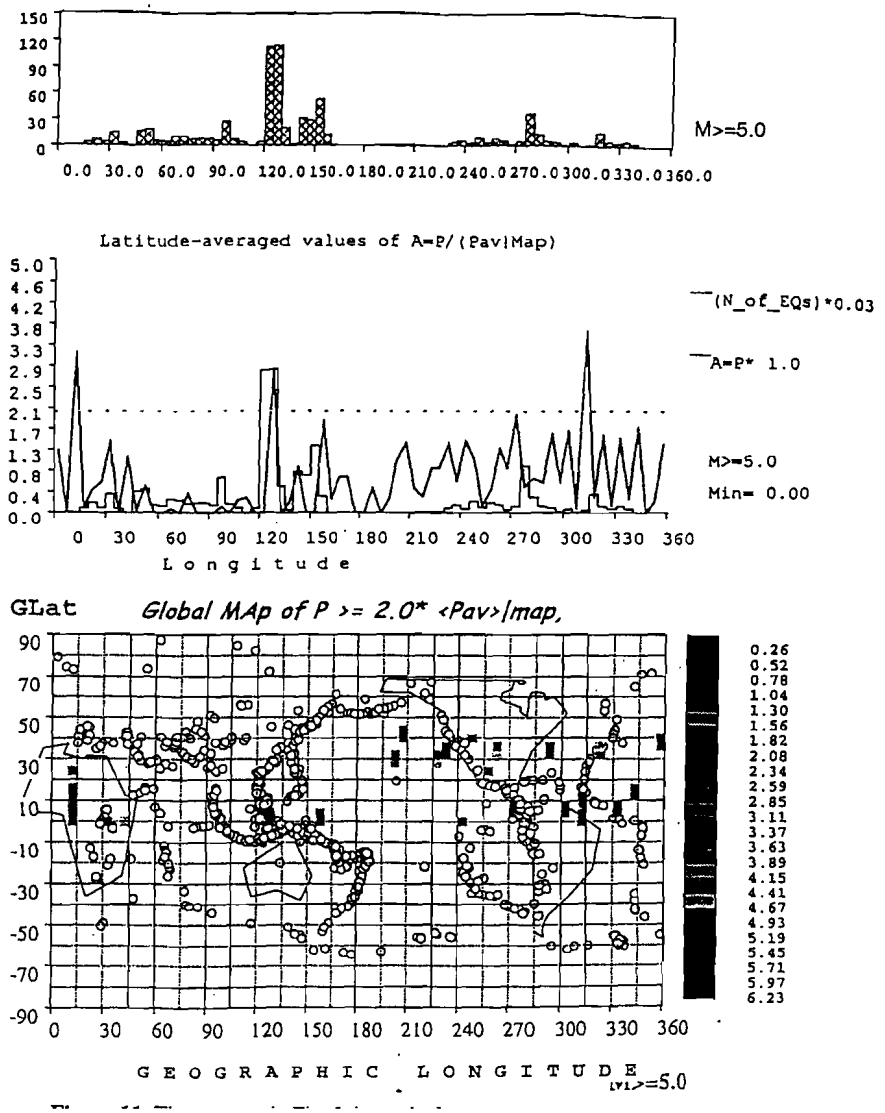

Fig. 11. The same as in Fig. 9, but only for the northern hemisphere.

planation of the facts presented in
nisphere are mainly controlled by
ssume an essential coupling along

Intercosmos-24 satellite we have
mos-900 satellite. Though we are

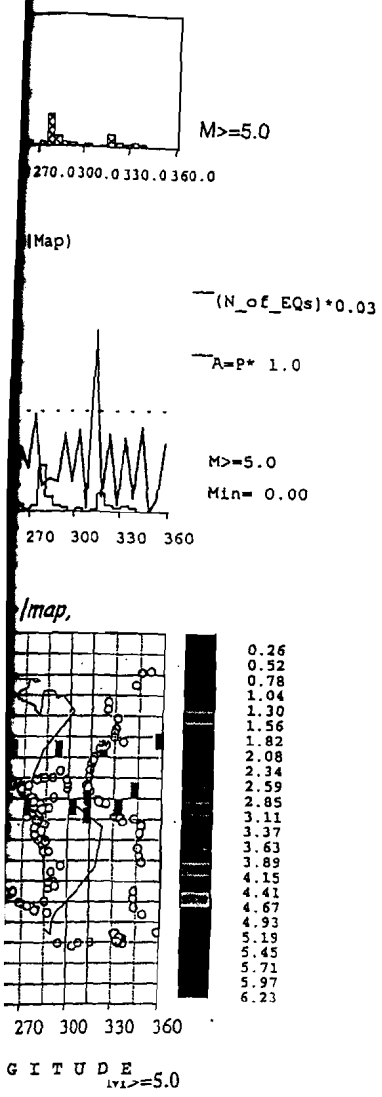

for the northern hemisphere.

going to discuss these data in a separate paper, it is suitable to show one result which is obtained for the same conditions: day time, $K_p < 3$, near perigee altitudes, $H = 500$–600 km (Fig. 14). It was a great surprise for us to find the same 3 peaks in the longitudinal dependence of density variations, related with seismic activity, as in our previous pictures.

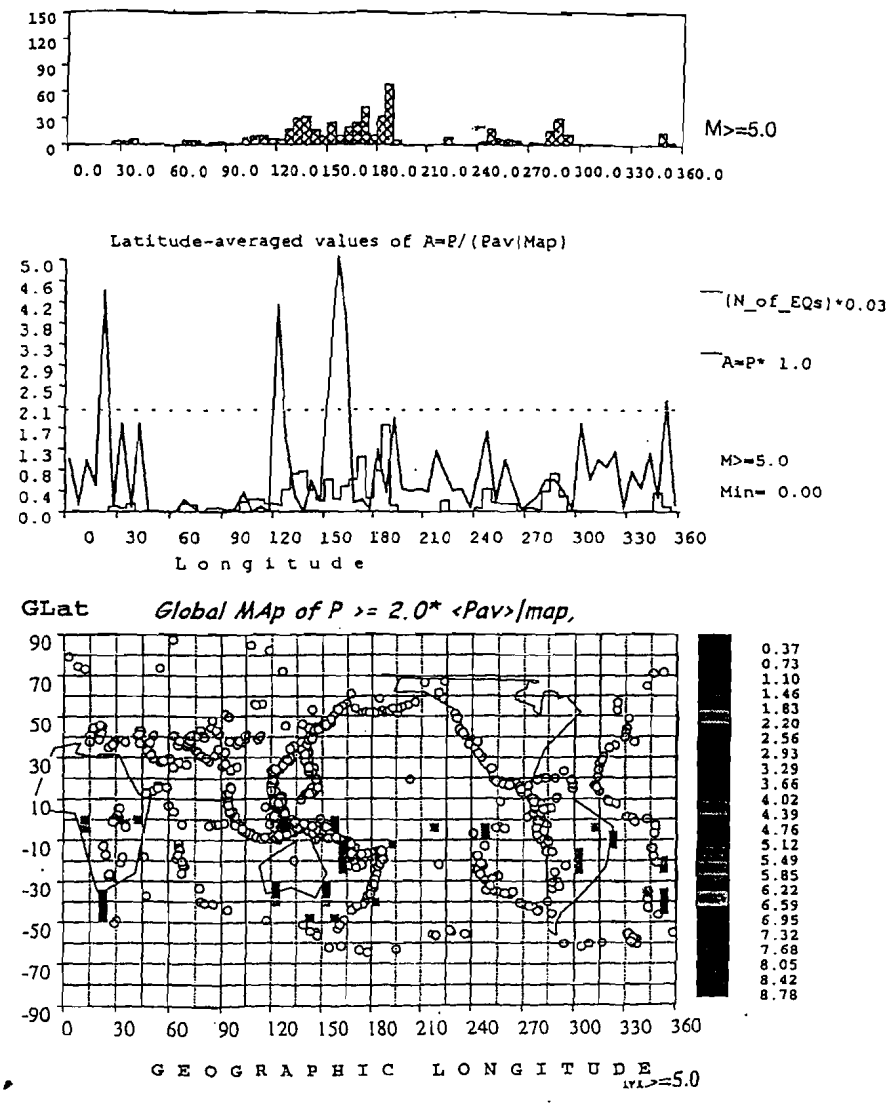

Fig. 12. The same as in Fig. 9, but only for the southern hemisphere.

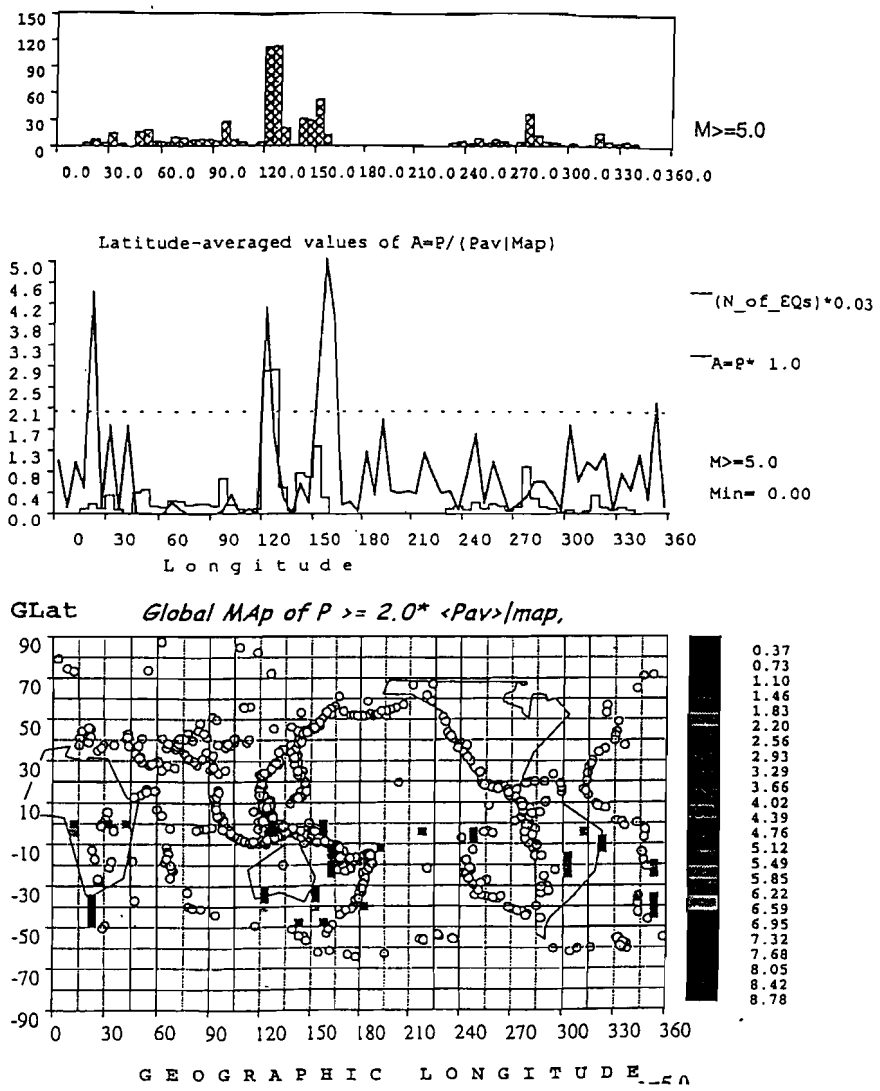

Fig. 13. The same as Fig. 12, but earthquake occurrence is given for the northern hemisphere, though RNSD is presented for the southern hemisphere.

Fig. 14.

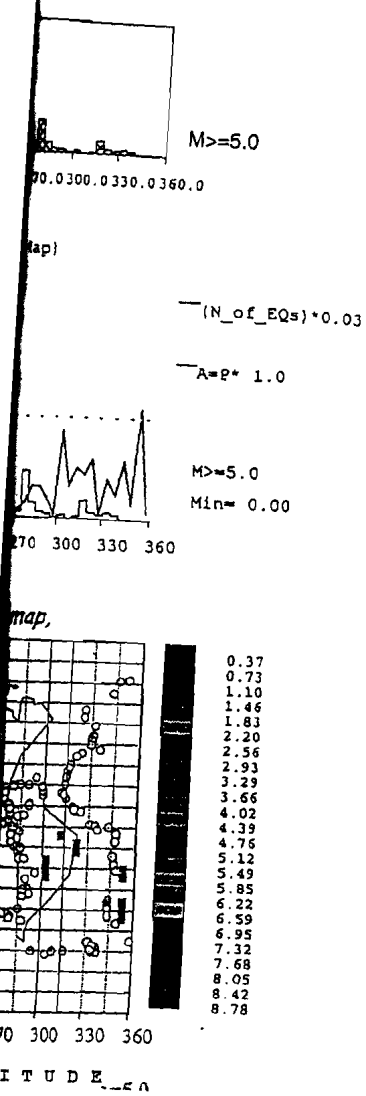

given for the northern hemisphere, though

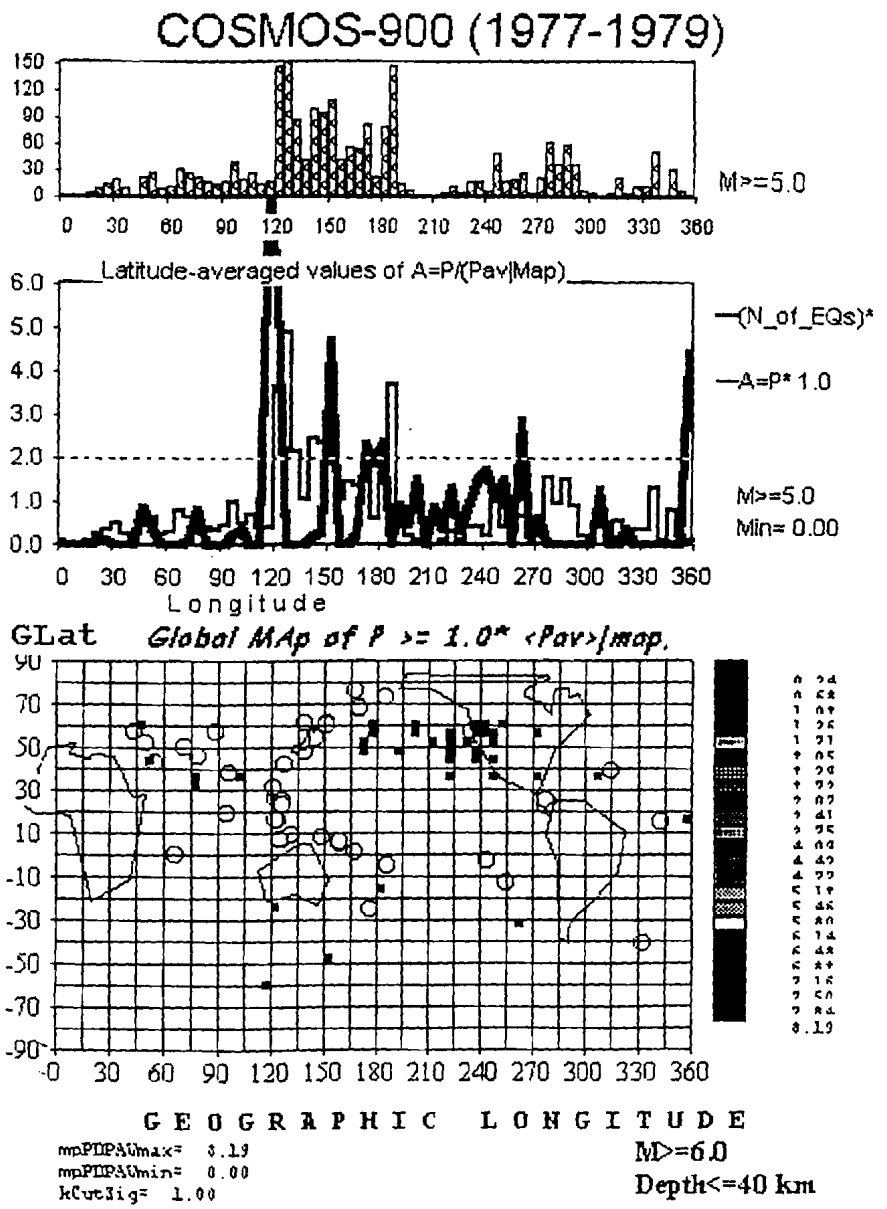

Fig. 14. Longitudinal dependence of earthquake occurrence rate and RNSD for the satellite Cosmos-900. Construction of plots is the same as for Intercosmos data.

4. Conclusions and Discussion

1. It seems that our finding has proven an existence of seismic influence onto the ionospheric plasma. Reliability of this proof is justified by using the 2σ criterion in classical statistics and visual peak to peak correlation of seismic occurrence and normalized density variations (Figs. 9–11, 13–14). It is easy to estimate that correlation coefficient of two plots in these figures in a range $\lambda \sim$ 110–190° is better than 0.6–0.8.

2. The effect is very sensitive to conditions of observation and the finding is successful only after several limitations. Some of these limitations are evident, e.g. limitation on K_p and latitude. Selection of day time might be related with a better stability of density behavior during the interval LT = 10–16. It is difficult to explain an altitude limitation (ΔH = 500–700 km). Probably, this layer of ionosphere between the main ionospheric maximum below and ion transition heights above is the most "quiet" to natural perturbations. Anyway, one important and practical consequence of our finding is the following: if we would like to measure the seismogenic plasma perturbations on satellites, it is desirable to choose a circular orbit at altitude 500–700 km.

Table 3. Data capacity around earthquake time ±30 days, LT = 10–16, $K_p < 3$, H = 600–700 km.

Num	Index	Lat., deg	Long. Deg	Depth., km	Magn	Time(UT) - Date	N points	<N> per cell
1	Z 1	5.0	32.1	7	6.6	02.21-20.05.90	5776	1.8
2	Z 2	15.7	121.2	25	6.6	07.26-16.07.90	3159 (67824)*	1.0 (20.9)*
3	Z 4	9.7	276.9	10	6.6	21.56-22.04.91	10123	3.1
4	Z 5	30.7	78.8	19	6.5	21.23-19.10.91	3907	1.2
5	Z 6	4.6	282.5	21	6.5	22.28-19.11.91	1618	0.5
6	Z 4a	39.4	144.8	10	6.4	13.09-07.05.91	10168	3.1
7	Z 4b	42.1	234.4	10	6.4	02.50-13.07.91	8880	2.7
8	Z 2b	53.5	169.9	32	6.4	20.14-06.11.90	1245	0.4
9	Z 1a	37.0	49.4	10	6.3	21.00-20.06.90	2433 (69502)*	0.8 (21.4)*
10	Z 2a	41.6	88.8	0	6.2	04.59-16.08.90	1427	0.4
11	Z 3	- 6.0	282.9	33	6.5	04.19-05.04.91	10869	3.4

*Number of points for all the range of altitudes (see text).

3. Geomagnetic control of the seismo-ionosphere coupling is found (Figs. 11–13). Though the mechanisms of seismic influence on the plasma of upper ionosphere are not clear, this fact should be included in any future theoretical explanations.

4. As concerned with the possibility of a case study, the situation became better because we are sure now that a seismogenic effect exists. On the other hand, selection of appropriate conditions to observe it, could be sometimes a difficult job. To demonstrate a real situation we have made a special listing around the times of the largest earthquakes during the operation of Intercosmos-24 satellite. Five columns in this table are parameters of earthquake: latitude, longitude, depth, magnitude and date. Sixth column is number of observational points, obtained during the temporal interval ±30 days around the moment of the earthquake, during day time (LT = 10–16), $K_p < 3$ and at the altitude range 600–700 km. Seventh column is average number of points in elementary cell 4×5 degrees above the earthquake epicenter. This number is too small for the reliable statistics, even when we have observed large perturbations of density in comparison with average ones. Consequently, we need either to relieve our limitation and to worsen a sensitivity or to use a more suitable satellite. For example if we consider all the range of altitudes, the number of points in Table 3 will increase by 20–30 times and will be possible to find a convincing earthquake signature. That is why we need a satellite with the circular orbit.

5. In conclusion, at present we have only proved a feasibility of satellite monitoring for seismic activity. In order to estimate an efficiency of such observations we would like to continue our research using other types of data and different criteria of their discrimination.

REFERENCES

(1) Hayakawa, M. and Y. Fujinawa, "*Electromagnetic Phenomena Related to Earthquake Prediction*", Terra Sci. Pub. Comp., Tokyo, pp. 677, 1994.

(2) Molchanov, O. A., Wave and Plasma Phenomena inside the Ionosphere and Magnetosphere Associated with Earthquakes, *The Review of Radio Science, 1990–1992*, ed. by W. R. Stone, Oxford Univ. Press, 591–600, 1993.

(3) Molchanov, O. A., M. Hayakawa and T. Kodama, Earthquake pattern from seismic and geophysical observations on the ground and its reflection into the atmosphere and ionosphere, *Abstracts of Int'l Workshop on Seismo Electromagnetics*, Chofu, March 3–5, 1997, p. 78, 1997.

(4) Hayakawa, M., Electromagnetic Precursors of Earthquakes: Review of Recent Activities, *The Review of Radio Science, 1993–1995*, ed. by W. R Stone, Oxford Univ. Press, 1996.

al.

existence of seismic influence onto proof is justified by using the 2σ eak to peak correlation of seismic s (Figs. 9–11, 13–14). It is easy to lots in these figures in a range $\lambda \sim$

ions of observation and the finding me of these limitations are evident, of day time might be related with a interval LT = 10–16. It is difficult –700 km). Probably, this layer of naximum below and ion transition rturbations. Anyway, one important the following: if we would like to ons on satellites, it is desirable to m.

ys, LT = 10–16, $K_p < 3$, H = 600–700 km.

Time(UT) - Date	N points	<N> per cell
02.21-20.05.90	5776	1.8
07.26-16.07.90	3159 (67824)*	1.0 (20.9)*
21.56-22.04.91	10123	3.1
21.23-19.10.91	3907	1.2
22.28-19.11.91	1618	0.5
13.09-07.05.91	10168	3.1
02.50-13.07.91	8880	2.7
20.14-06.11.90	1245	0.4
21.00-20.06.90	2433 (69502)*	0.8 (21.4)*
04.59-16.08.90	1427	0.4
04.19-05.04.91	10869	3.4

(see text).